Energies **2015**, *8*, 7020-7039; doi:10.3390/en8077020

OPEN ACCESS

energies

ISSN 1996-1073

www.mdpi.com/journal/energies

Article

A Novel Ground Fault Identification Method for 2 × 5 kV Railway Power Supply Systems

Jesus Serrano, Carlos A. Platero *, Maximo López-Toledo and Ricardo Granizo

Department of Electrical Engineering, Escuela Técnica Superior Ingenieros Industriales, Technical University of Madrid, C/José Gutierrez Abascal, 2, Madrid 28006, Spain; E-Mails: jserranoalv@hotmail.com (J.S.); maximo.lopez.t@gmail.com (M.L.-T.); ricardo.granizo@upm.es (R.G.)

* Author to whom correspondence should be addressed; E-Mail: carlosantonio.platero@upm.es; Tel.: +34-91-336-31-29; Fax: +34-91-336-30-08.

Academic Editor: William Holderbaum

Received: 21 April 2015 / Accepted: 6 July 2015 / Published: 13 July 2015

Abstract: The location of ground faults in railway electric lines in 2 × 5 kV railway power supply systems is a difficult task. In both 1 × 25 kV and transmission power systems it is common practice to use distance protection relays to clear ground faults and localize their positions. However, in the particular case of this 2 × 25 kV system, due to the widespread use of autotransformers, the relation between the distance and the impedance seen by the distance protection relays is not linear and therefore the location is not accurate enough. This paper presents a simple and economical method to identify the subsection between autotransformers and the conductor (catenary or feeder) where the ground fault is happening. This method is based on the comparison of the angle between the current and the voltage of the positive terminal in each autotransformer. Consequently, after the identification of the subsection and the conductor with the ground defect, only the subsection where the ground fault is present will be quickly removed from service, with the minimum effect on rail traffic. This method has been validated through computer simulations and laboratory tests with positive results.

Keywords: ground faults; protection; 2 × 25 kV; fault location; railways

---

1. Introduction

High-speed trains demand a power of about 12–16 MW to be able to reach speeds over 300 km/h. The normal method to provide such high levels of power comprises two power supply conductors and a grounded return one, which is called a 2 × 25 kV traction system, although there are other power supply systems with differently rated voltages [1].

This power supply system has a positive conductor (usually called catenary) at 25 kV AC voltage with a positive polarity with respect to ground, and a negative voltage conductor (usually called feeder) at 25 kV AC voltage with a negative polarity with respect to ground. The supply to the trains employs the catenary and the grounded rail.

In these power systems, the complete traction line is supplied by several traction substations (TS). Each traction substation supplies two sections. Moreover, in each section, there are several subsections at regular intervals which are delimited by stations with power autotransformers (ATS). The autotransformer terminals are connected to the catenary and feeder, whereas its middle winding point is connected to the rail. At the end of each section another autotransformer station (SATS) is installed, where an autotransformer is connected in a similar way. In Figure 1, a traction line section with three sub-sections is shown, as well as the theoretical current distribution.

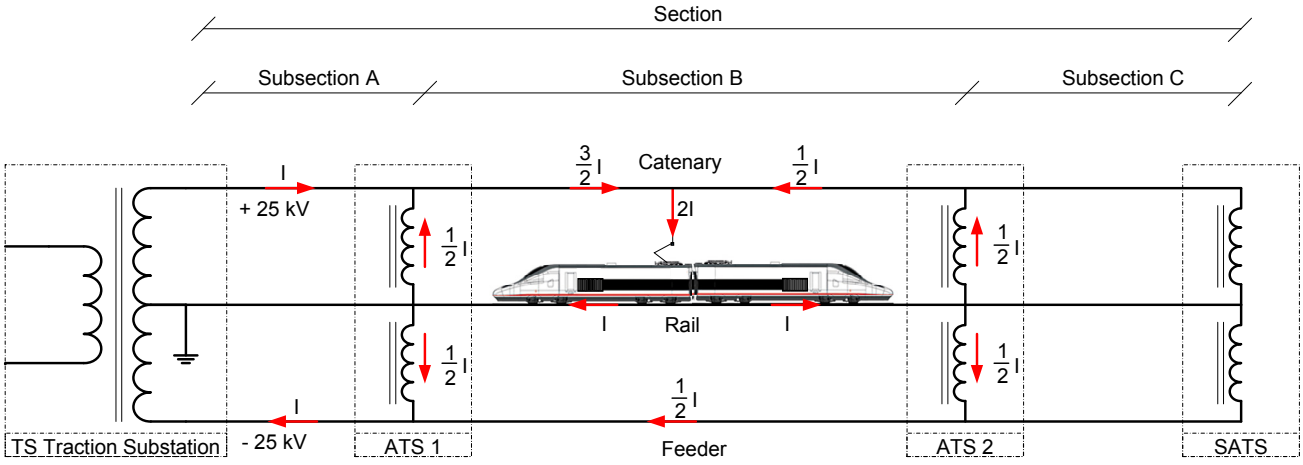

Figure 1. Simplified diagram of a 2 × 25 kV power system and current distribution in a section comprising three subsections.

In 2 × 25 kV power systems, the traction power demanded is delivered at 50 kV while it is used at 25 kV. This fact reduces the current needed to supply the power required by high-speed trains [2]. In consequence, as this configuration presents lower losses and voltage drops along the line in comparison to 1 × 25 kV substation topologies, the length of the sections can be greater and the number of traction substations lower.

Another remarkable advantage of the 2 × 25 kV traction systems is the great reduction of electromagnetic interference on communication facilities and railway signalling circuits (signalling track circuits) as well as in nearby telecommunication lines [3,4].

Protection systems are essential to ensure the safe and efficient operation of any electrical installation [5,6]. Also, the proper management of these systems is an important factor to take into account in the profitability of these facilities [7].

All electrical systems, especially railway traction systems, can have internal failures of their equipment and external faults caused by accidental events. Furthermore, in the traditional 1 × 25 kV power supply systems, most faults are caused by outdoor short circuits between the catenary and ground, while in the 2 × 25 kV power systems most of them are caused by outdoor short circuits between the catenary or the feeder to ground [8,9]. However, the detection and location of ground faults in the 2 × 25 kV lines are much more complex than in 1 × 25 kV lines, mainly because of the use of autotransformers [10] in the ATS substations to which the catenary, feeder and rails are connected.

The complexity of the detection and location of ground faults in the 2 × 25 kV lines means that the identification of the subsection and the conductor where the ground fault has happened [11,12] is the main task of the protection systems in order to disconnect immediately the conductor with the ground fault in the corresponding subsection [13]. This means only trains running in the subsection with the ground fault, in the case that the fault is in the catenary, will be disconnected from the power supply.

This paper describes a new method for identifying the subsection and the conductor (catenary or feeder) in which there is a ground fault in an easy and economical way. As the identification is done immediately, the subsection and conductor can be disconnected while keeping the rest of the power system in service. Another important advantage is that most of the elements that this method needs to be operative are already installed in any 2 × 25 kV power supply system, and consequently little new investment is required.

This new method has been validated through numerous computer simulations and experimental laboratory tests, obtaining excellent results. This paper first presents in Section 2 an overview of the problem of ground fault location in 2 × 25 kV power systems and a brief description of the current methods. Then, Section 3 details the principles of the proposed method, and Section 4 presents an analysis of the simulations developed with MATLAB® software. Section 5 presents the results of experimental tests carried out in a laboratory set-up. Finally, Section 6 concludes with the main contributions of the proposed new technique.

2. Ground Fault Location in 2 × 25 kV Power Systems: Description of the Problem

In traction power systems with ATS's (2 × 25 kV), whose electrical scheme and current distribution are represented in Figure 1, as well as in single-phase (1 × 25 kV) power systems, the main protection system is normally based on distance protection relays [14]. These protection relays are usually installed at the traction substations and measure the impedance as the ratio between the voltage of the catenary and the difference of the catenary and feeder currents.

However, such traction power systems with ATSs (2 × 25 kV) do not make use of ground fault location based on the linear ratio between the impedance (Z) seen from the traction substation and the distance to the ground fault. This linear ratio, represented in Figure 2, does, however, allow the distance protection relays to detect the ground fault and calculate the distance to the defect [15–17] in one-conductor power systems (1 × 25 kV).

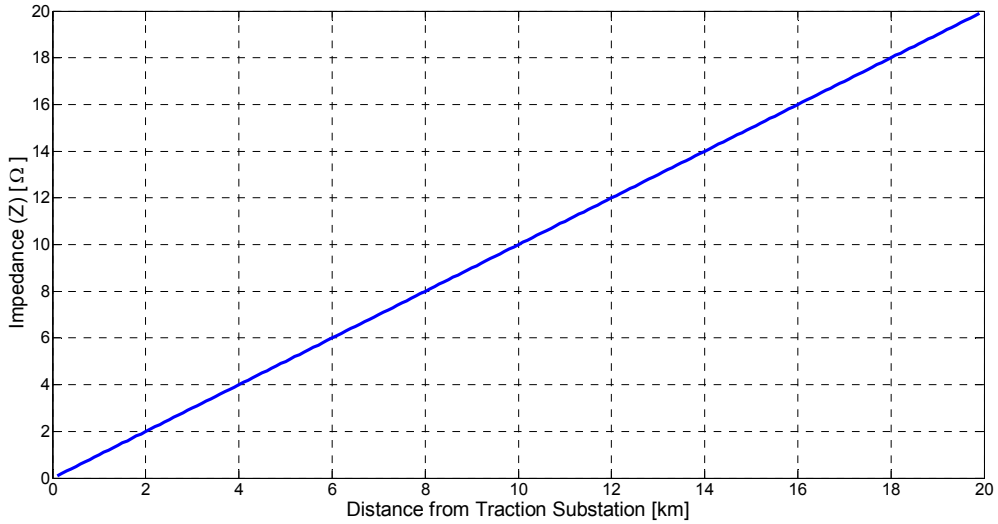

Figure 2. Modulus of the fault impedance (Z) seen from the traction substation as a function of the distance in 1 × 25 kV traction power systems.

However, in traction power systems with ATSs (2 × 25 kV), the variation of the impedance value measured as a function of the distance to the ground fault is non-linear [11,16]. Figure 3 shows the real values of the fault impedance measured, where it can be seen that the ratio is non-linear in every subsection between two ATSs. The minimum values of the impedance measured correspond to the ATS's emplacements.

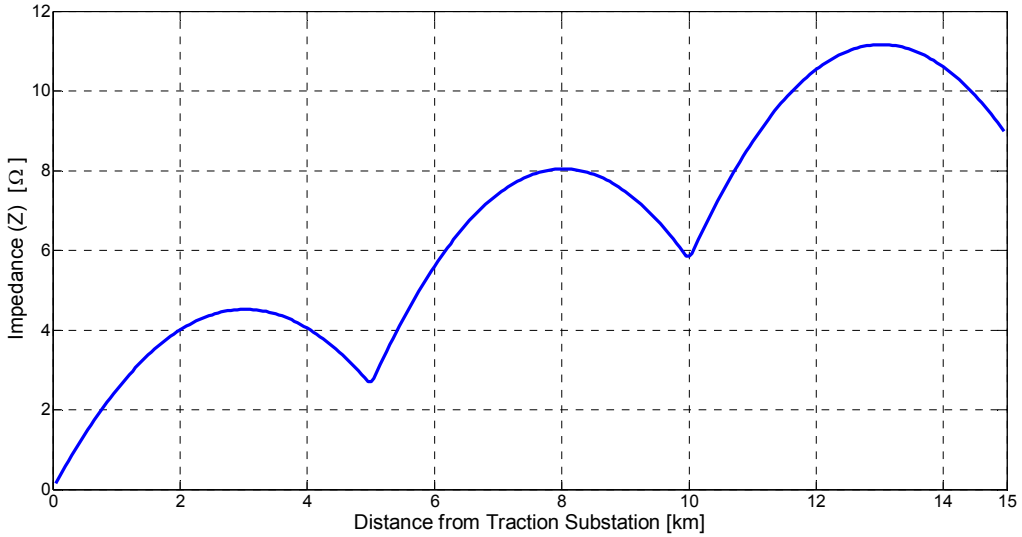

Figure 3. Modulus of the fault impedance seen from the traction substation in function of the distance in 2 × 25 kV traction power systems.

Figure 3 reveals clearly that only measuring the modulus of the impedance to the ground fault in a subsection does not allow the location of the fault to be identified. Even when the modulus of the impedance is known, it is not possible to define in which subsection between two ATSs the ground fault has occurred, because the same value of measured impedance can be obtained from different subsections. As a result, it is standard practice at railway facilities to follow the protocol described in the following paragraphs.

When a ground fault happens, the distance protection relays register an impedance value lower than their settings values and a tripping command is released to the normally used double pole circuit-breakers in the substation, with a consequent interruption of the power supply in all subsections and ATS's of the section with the defect.

After a pre-set time, the distance protection relays conduct automatic reclosing manoeuvres and again feed the subsections and ATSs, checking that the defect is not permanent. If the ground fault is still active, the distance protection relays switch off the circuit-breakers again and open the motor-driven disconnectors installed at the ATS's substations. The next step is to switch on the circuit-breakers again. Now, as the catenary and feeder conductors are electrically isolated (the system operates as 1 × 25 kV), the distance protection relays will allow the conductor where the ground fault took place to be identified, as well as the relatively accurate identification of the subsection [18].

To isolate the subsection with the ground fault, the information provided by the distance protection relay is used. As the circuits of the two conductors are now totally independent, the distance from the substation to the ground fault is obtained from the impedance measured by the distance protection relay. Once the subsection is isolated through its corresponding motor-driven disconnectors, the rest of the subsections without a ground fault are powered again. In the case of a lack of accuracy in the determination of the distance to the ground fault, a subsection which is closer to or farther away from the real distance to the fault may remain without power supply for an unacceptable time [19].

To avoid this delay in the isolation of the true subsection with the ground fault, it is very useful to know, as soon as the ground fault has been detected, in which subsection between ATSs this has taken place and if it happened in the catenary or feeder conductor. The new system presented in this paper allows us to know just after the ground fault which subsection has the ground defect and if the fault is located between the catenary and rail or between the feeder and rail conductors. As this information is sent to the control centre immediately, automatic or manual decisions can be taken to restore the power supply to the subsections without any ground fault.

3. Principles of the New Ground Fault Subsection Identification Method

According to the theoretical current distribution of 2 × 25 kV power system (Figure 1), the phase angle between voltage and current in the autotransformer is close to 180° in case of resistive load (Figure 4a). In this case, the catenary inductance (X_L) can be neglected.

On the other hand, in case of an inductive load the phase angle between voltage and current in the autotransformer is close to 90°, as shown in the Figure 4b.

The power factor of the high-speed trains is close to the unit; therefore, the current distribution under normal operation of a 2 × 25 kV power system is similar to the resistive load case shown in Figure 4a.

The catenary short-circuit current is similar to the inductive load case, as the impedance seen from the autotransformer is the catenary inductance X_L. (Figure 4c).

Finally in the Figure 4d the feeder short-circuit case is represented, and it is symmetrical to the above case.

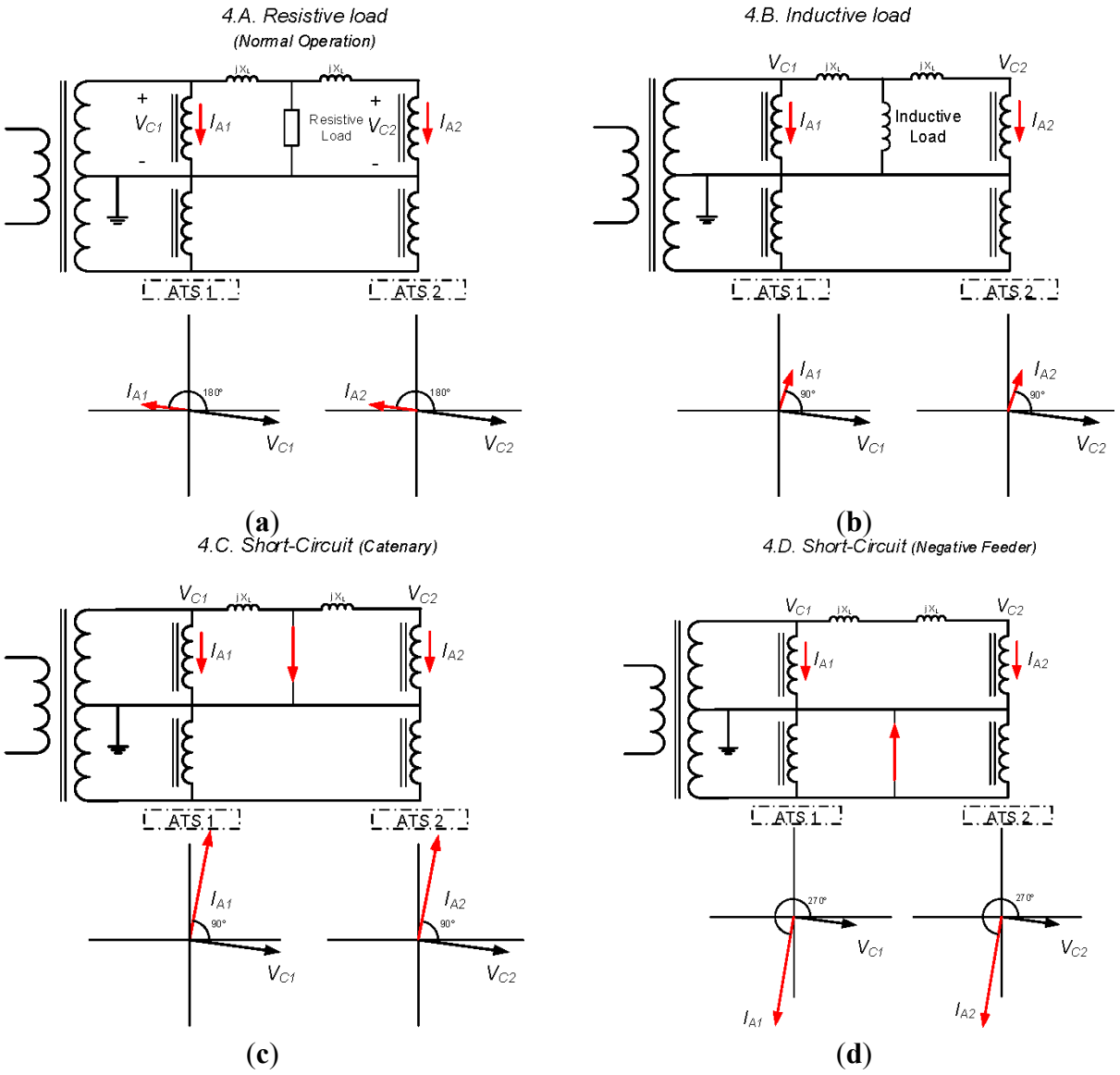

Figure 4. 2 × 25 kV theoretical currents distribution in case of resistive load (**a**); inductive load (**b**); short-circuit (catenary) (**c**); and short-circuit (negative feeder) (**d**).

When there is a ground fault on a line between the catenary and rail or between the feeder and rail in a 2 × 25 kV traction power system, there is a substantial increase in the current circulating through the windings of the ATSs closest to the defect location. This current increase can be detected easily by measuring the currents in the windings of the ATSs. Furthermore, when the fault happens, the angles between the currents and voltages change in the ATSs closest to the fault location.

In normal operation, these angles between the currents and voltages in the autotransformers are close to 180°, as shown in Figure 5. On the other hand, in the case of a ground fault, the phase angle between the voltage and current in the autotransformers will shift by 90°, as will be shown later.

As an example, we can consider a ground fault in subsection C as shown in Figure 6, where the modulus of the currents IA2 and IA3 increase their value by a great deal, whereas the current IA1 does not undergo any remarkable change in its value.

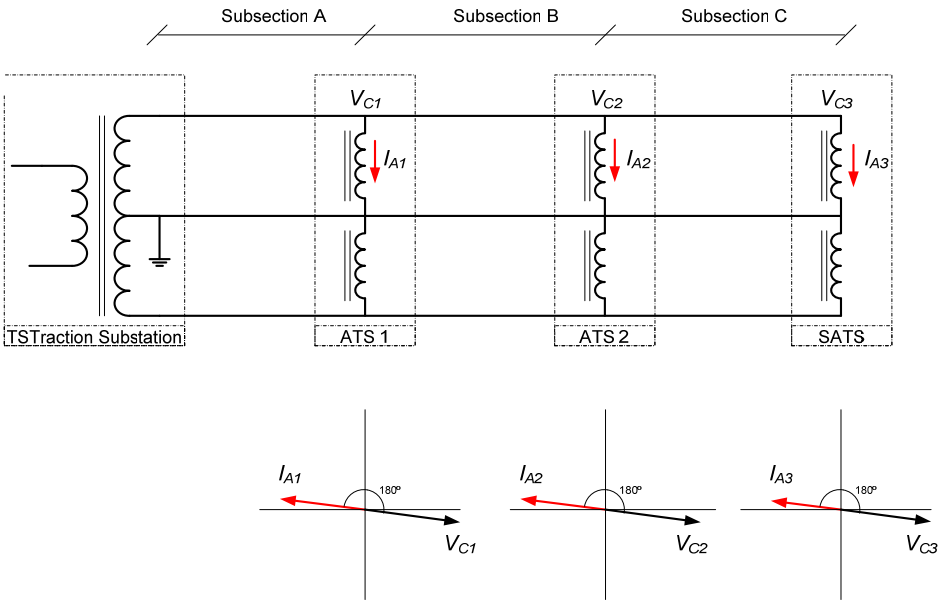

Figure 5. 2 × 25 kV power system currents (I_A) and voltages (V_C) distribution in normal operation.

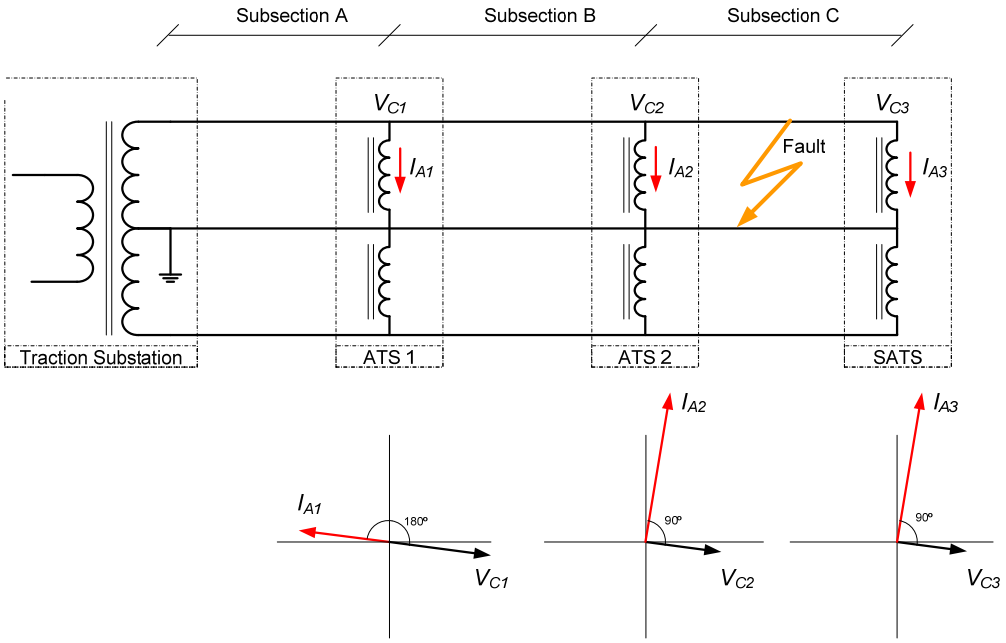

Figure 6. 2 × 25 kV power system currents (I_A) and voltages (V_C) distribution with a ground fault in the catenary in Subsection C.

Furthermore, the angles between such currents I_{A2} and I_{A3} and the respective catenary to rail voltages V_{C2} and V_{C3} will change dramatically. In this case, as the fault is between the catenary and the rail in Subsection C, the angle between I_{A2} and V_{C2} changes in value from approximately 180° to 90° (see Figures 5 and 6).

The angle between I_{A3} and V_{C3} is also reduced from close to 180° to near 90°. As indicated before, the angle between I_{A1} and V_{C1} remains stable with almost no variation, as can be seen in Figure 6.

Now, if the ground fault happens in the same Subsection C but between the feeder and rail, the angle between I_{A2} and V_{C2} changes from 180° to 270° (see Figures 5 and 7). There is also the same angle change between I_{A3} and V_{C3}. Again, there is no significant change in the angle between I_{A1} and V_{C1}.

If the ground fault happens in Subsection B, the current increase will affect only currents I_{A1} and I_{A2} and there will be no remarkable change in current I_{A3}. The angles between I_{A1} and V_{C1}, and I_{A2} and V_{C2} respectively will change, but not the angle between I_{A3} and V_{C3}. These phase angle changes will also be from 180° to 90° in the case of a fault between the catenary and rail (see Figures 5 and 8), and from 180° to 270° if the fault is between the feeder and rail.

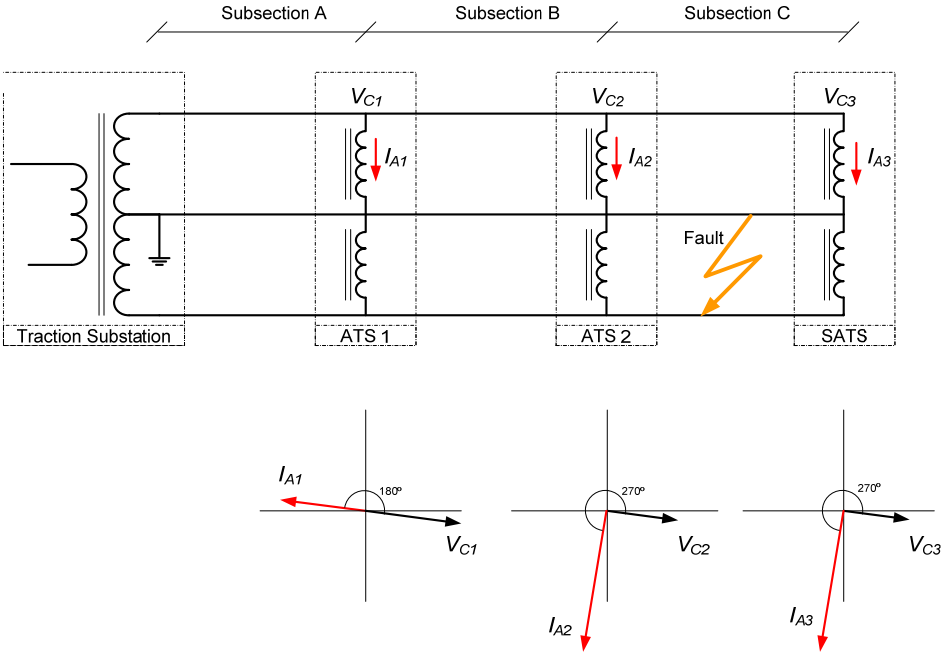

Figure 7. 2 × 25 kV power system current (I_A) and voltage (V_C) distribution with a ground fault in the feeder in subsection C.

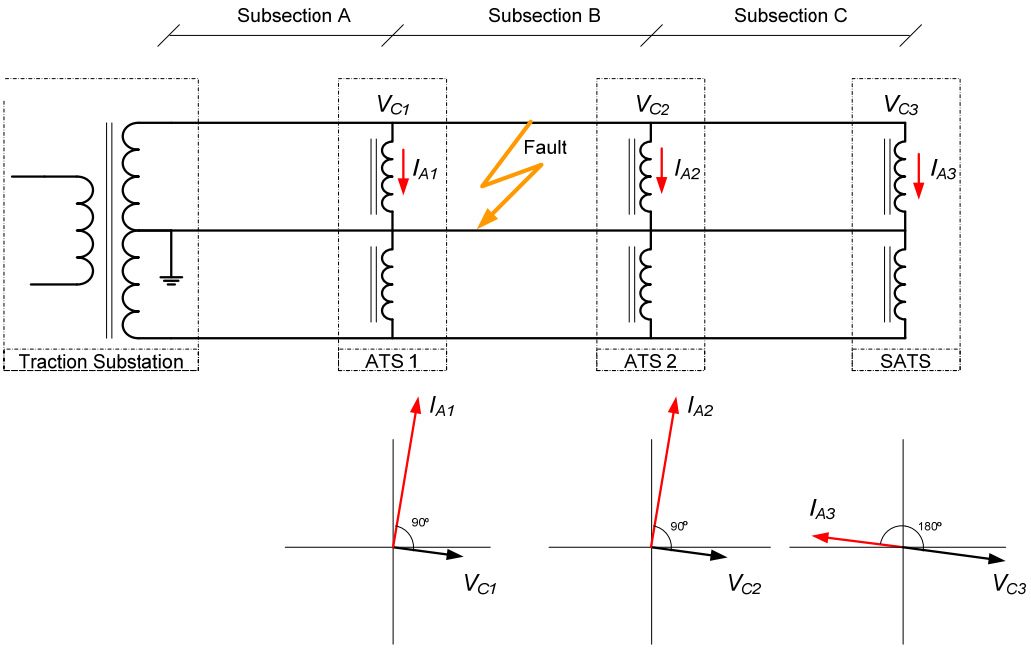

Figure 8. 2 × 25 kV power system currents (I_A) and voltages (V_C) distribution with a ground fault in the catenary in subsection B.

However, if there is a ground fault in Subsection A, only the current I_{A1} increases in value, while currents I_{A2} and I_{A3} remain stable with no significant changes in their values. Therefore, the change in the phase angle only affects the current I_{A1} and voltage V_{C1}, but not the currents and voltages in the ATS2 and SATS. This variation in the phase angle between the current and voltage in the ATS1 installed at the end of the first subsection indicates that the ground fault is located in the first Subsection A.

In fact, in facilities whose sections have more than two subsections, it is possible to avoid taking measurements at the station with ATS situated at the end of the last subsection (SATS). This is because when there is a current increase and a variation of the angle between the current and voltage only in the previous ATS (ATSN-1), the ground fault is located in the last subsection N. Figure 9 represents a section formed by N subsections (with N > 2) with measuring devices for current and voltage in all stations with ATSs except in the last one (SATS).

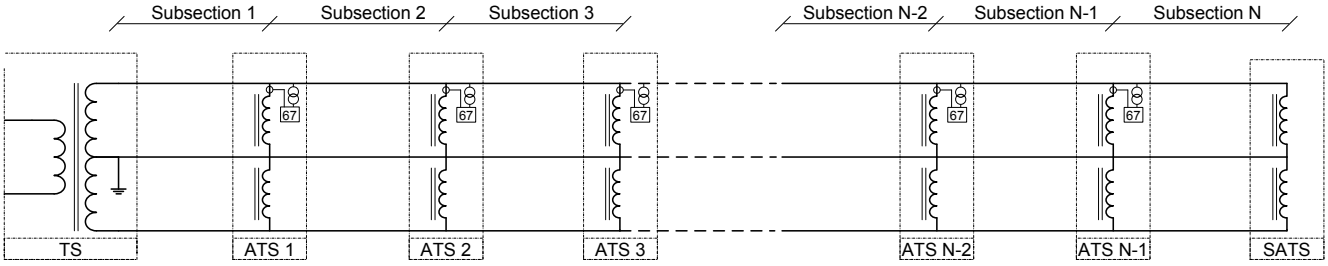

Figure 9. Section with N subsections supplied from the traction substation (TS) with N-1 measurement devices for current and voltage.

The changes of the angle between the currents and voltages when there is a ground fault in the system represented in Figure 9 are listed in Table 1.

Table 1. Angle variation between I_A and V_C as a function of the subsection with the ground fault.

Fault location	ATS1	ATS2	ATS3	ATSN-3	ATSN-2	ATSN-1
Fault at catenary in Subsection 1	90°	180°	180°	180°	180°	180°
Fault at feeder in Subsection 1	270°	180°	180°	180°	180°	180°
Fault at catenary in Subsection 2	90°	90°	180°	180°	180°	180°
Fault at feeder in Subsection 2	270°	270°	180°	180°	180°	180°
Fault at catenary in Subsection 3	180°	90°	90°	180°	180°	180°
Fault at feeder in Subsection 3	180°	270°	270°	180°	180°	180°
Fault at catenary in Subsection N-3	180°	180°	180°	90°	180°	180°
Fault at feeder in Subsection N-3	180°	180°	180°	270°	180°	180°
Fault at catenary in Subsection N-2	180°	180°	180°	90°	90°	180°
Fault at feeder in Subsection N-2	180°	180°	180°	270°	270°	180°
Fault at catenary in Subsection N-1	180°	180°	180°	180°	90°	90°
Fault at feeder in Subsection N-1	180°	180°	180°	180°	270°	270°
Fault at catenary in Subsection N	180°	180°	180°	180°	180°	90°
Fault at feeder in Subsection N	180°	180°	180°	180°	180°	270°

If the variation of the phase angle between the current and voltage only takes place at the ATSN-1 installed between Subsections N and N-1, the ground fault is located in Subsection N. It is also observed that if the variation of such angle only happens in ATS1, the ground fault is in Subsection 1. Therefore, if variation of the angles between currents and voltages occurs in two ATS's, the ground fault is in the subsection delimited by those ATS's.

In the case that a section only has two subsections, it is also necessary to measure the currents and voltages at the installed end autotransformer SATS. If so, when there is only a variation in the angle between the current and voltage in ATS1, the ground fault is in the first subsection, and if the fault occurs in the second subsection, the angle variation happens at both ATS1 and SATS.

If the angle is measured between the incoming current from the feeder in the winding of each ATS and catenary voltage V_C, in the case of a fault between the catenary and rail, this angle will be 270°, whereas if the fault is located between the feeder and rail, this angle will now be 90°. This angle situation is exactly the opposite when the incoming current in the winding of each ATS from the catenary is measured.

4. Experimental Simulations

In order to check the validity of the fundamentals of the proposed new method, numerous simulations were carried out using MATLAB® software. For this purpose, the circuit shown in Figure 10 was programmed using the modified nodal circuit analysis method [20]. The experimental circuit is supplied from one end with two 25 kV AC sources with reverse polarity in each one. This circuit has three parts, A, B and C, each with a length of 10 km

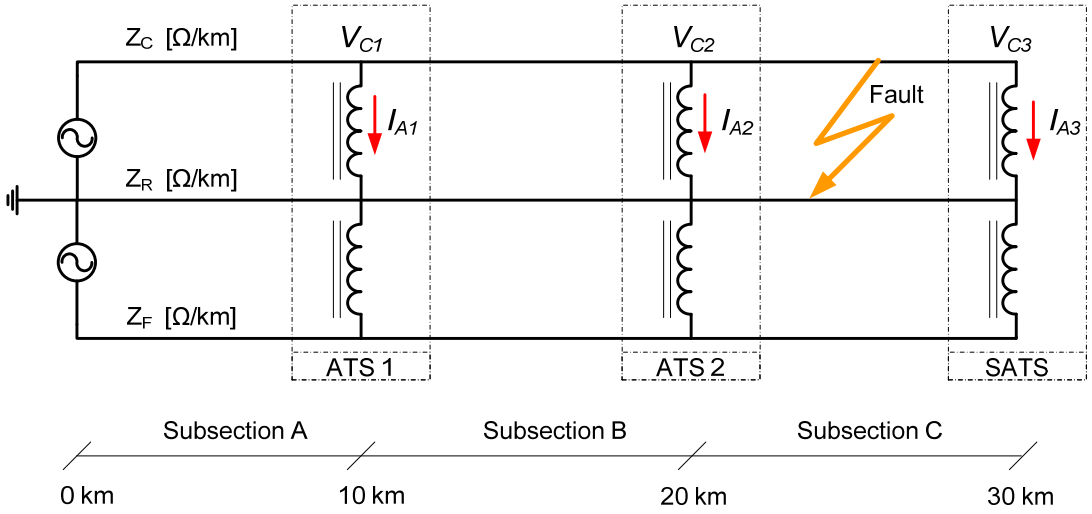

Figure 10. Simulated power supply system with two conductors and return grounded wire 2 × 25 kV.

To obtain the self-impedance values per length unit of the catenary Z_C, the feeder Z_F and rail connected to ground Z_R, as well as the mutual impedances between the conductors Z_{CR}, Z_{FR} and Z_{CF}, a new ATP software model was developed, including the geometry of the railway with five conductors. This ATP software model is shown in Figure 11 and uses resistance values per length unit as listed in Table 2. With such data incorporated into the ATP model, the impedance values obtained are given in Table 3.

Table 2. Resistance values of the railway per length unit.

Conductor	Resistance Ω/km
Contact wire (C.W.)	0.115
Messenger wire (M.W.)	0.172
Negative feeder (N.F.)	0.062
Aerial ground conductor (A.G.C)	0.119
Rails	0.026

Table 3. Self and mutual impedances values of the railway conductors.

Conductor		Impedance Ω/km
Catenary	Z_C	0.1197 + j0.6224
Feeder	Z_F	0.1114 + j0.7389
Rail	Z_R	0.0637 + j0.5209
Conductors		**Impedance Ω/km**
Catenary-Feeder	Z_{CF}	0.0480 + j0.3401
Catenary-Rail	Z_{CR}	0.0491 + j0.3222
Feeder-Rail	Z_{FR}	0.0488 + j0.2988

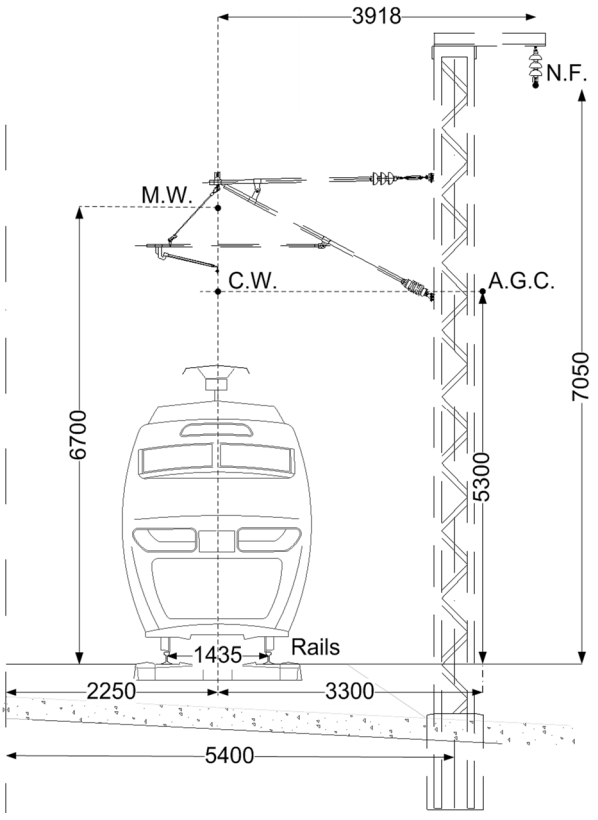

Figure 11. Railway geometry used for the model developed in ATP software (distances in mm).

These data obtained from the ATP railway model were implemented in the circuit shown in Figure 10. Employing this circuit, different MATLAB® simulations were developed, performing short-circuits between the catenary and rail, and between the feeder and rail. These short-circuits were simulated at all the points along the three Subsections A, B and C of the 30 km section. The phase angles between the currents I_{A1}-I_{A2}-I_{A3} and the voltages V_{C1}-V_{C2}-V_{C3} in the autotransformers ATS1, ATS2 and SATS,

as a function of the distance from the traction substation where the fault has happened between the catenary and rail, are represented in Figure 12. The axes used in Figure 12 are scaled from 0 to 30 km and from 0° to 360°. It can be observed that if the fault happens in Subsection A along the first 10 km, the angle between the current I_{A1} and voltage V_{C1} in the ATS1 is about 90°. However, such angles at ATS2 and SATS are 180°. Likewise, if the fault is in Subsection B (between 10 and 20 km) the phase angles between the current I_{A1} and the voltage V_{C1}, and between the current I_{A2} and the voltage V_{C2}, will be about 90° at both ATS1 and ATS2, while at SATS this angle is close to 180°. It can also be seen that if the fault is in Subsection C (between 20 and 30 km), the angle is about 90° at ATS2 and SATS but 180° at ATS1.

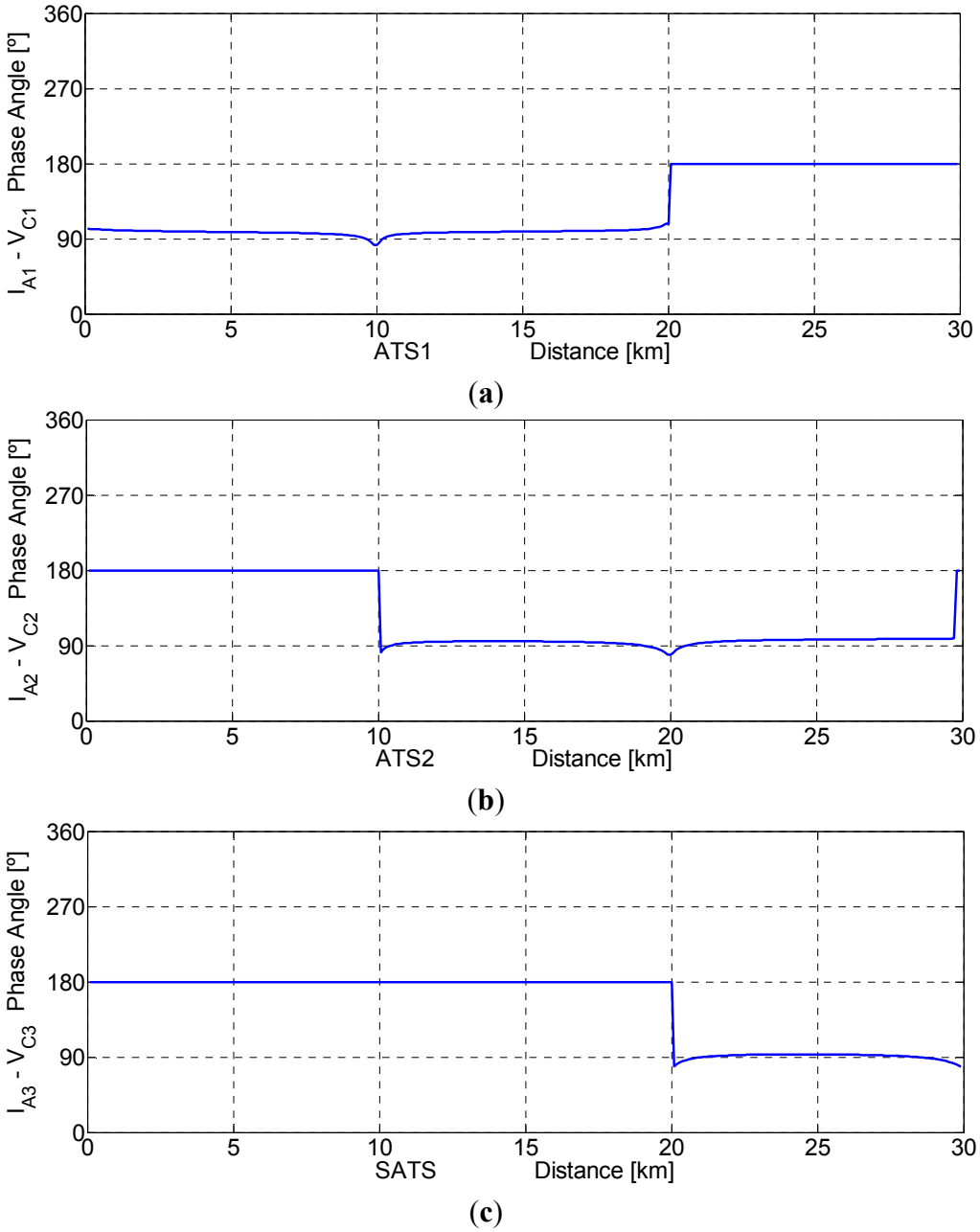

Figure 12. Phase angles between I_A and V_C at different ATSs as a function of the distance to the fault from the substation. Fault considered between catenary and rail. ATS1 (**a**); ATS2 (**b**) and SATS (**c**).

In the case that the fault happens between the feeder and rail, as expected in the theoretical research, the results obtained are similar when the fault takes place between the catenary and rail, except that now the angles between the currents I_{A1}-I_{A2}-I_{A3} and the voltages V_{C1}-V_{C2}-V_{C3} are 270° instead of 90°. Figure 13 shows how the variations of these phase angles as a function of the distance to the fault from the substation follow the same pattern as in the case of a fault between the catenary and rail, but now with values close to 270°.

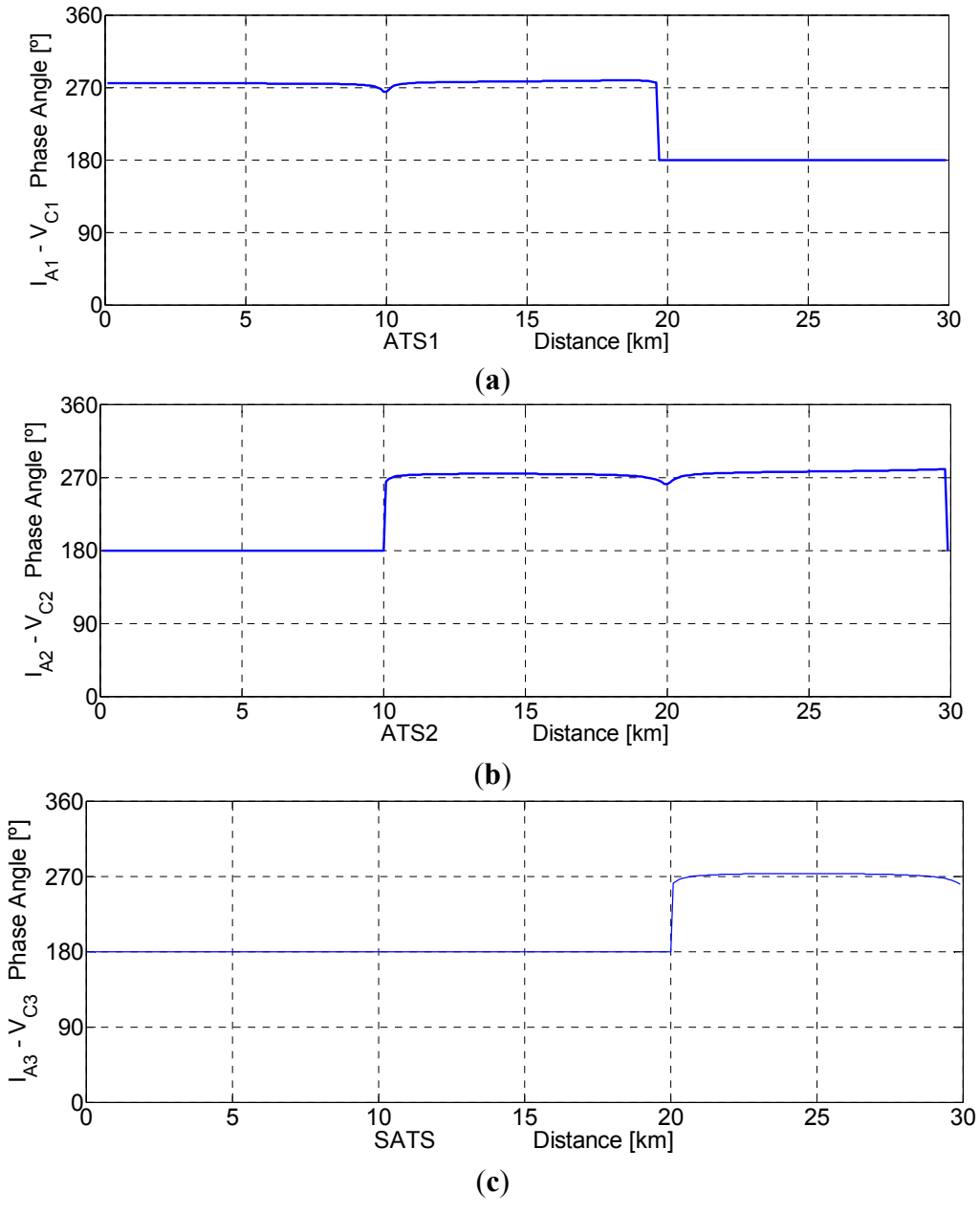

Figure 13. Phase angles between I_A and V_C at different ATS's as a function of the distance to the fault from the substation. Fault considered between feeder and rail. ATS1 (**a**); ATS2 (**b**) and SATS (**c**).

The results obtained from all the simulations developed confirm the theoretical values listed in Table 1, and therefore the identification of the conductor and subsection with the ground fault is totally successful.

5. Experimental Laboratory Tests

Besides the computer simulations, multiple tests were performed in the laboratory with the aim of getting, in a practical way, results that allow the identification of the conductor and subsection with the ground fault. These tests followed the circuit configuration indicated in Figure 14.

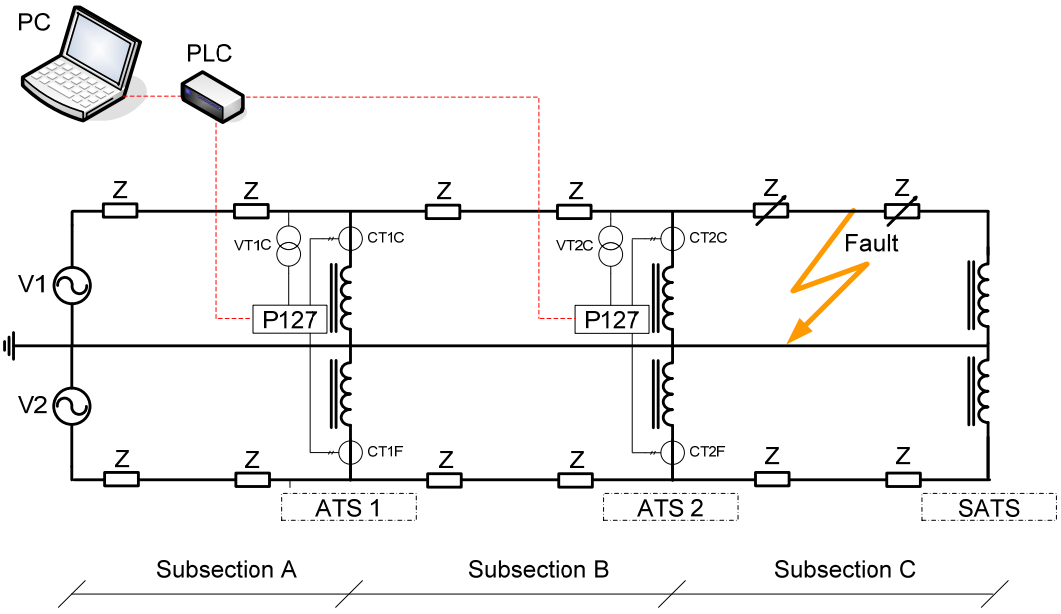

Figure 14. 2 × 25 kV experimental set-up of simplified circuit (one section with three subsections).

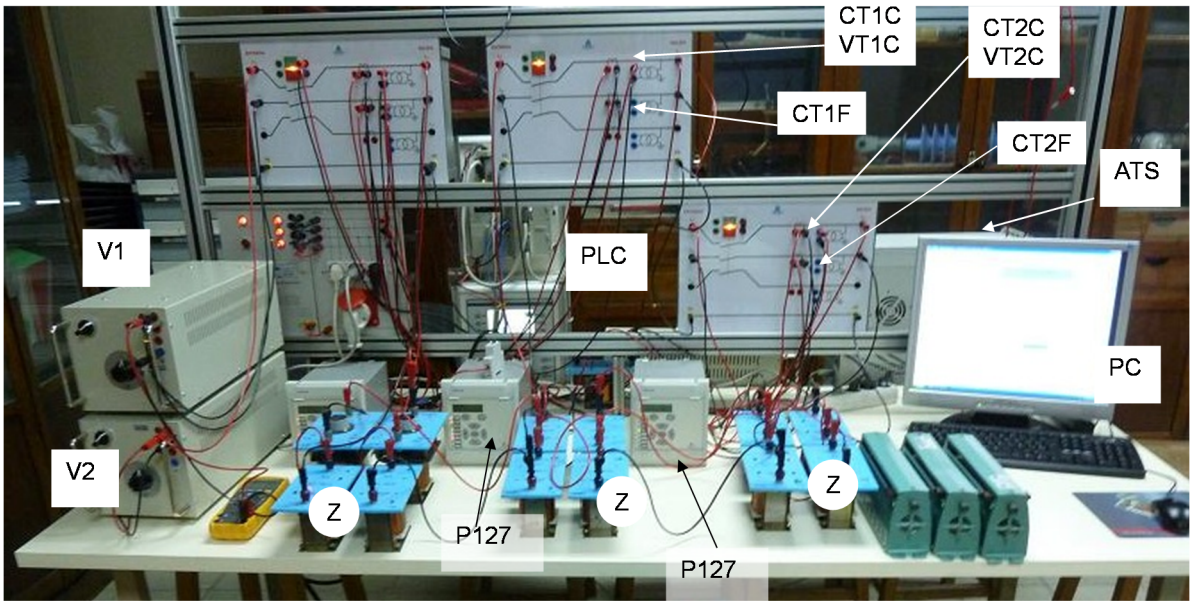

Figure 15. Experimental set-up circuit to simulate ground faults in laboratory.

The distributed impedance of the catenary and feeder was achieved using inductive impedances Z and two voltage sources, V1 and V2, supplying 100 V.

The section was divided into three Subsections A, B and C through ATS's. At the intermediate ATS's only (ATS1 and ATS2), measurement and control devices were installed: voltage transformers (VT1C and VT2C) were connected between the catenary and the 0 V conductor, current transformers

(CT1C and CT2C) were installed in the winding of the ATSs connected to the catenary, current transformers (CT1F and CT2F) were installed in the winding of the ATSs connected to the feeder, and directional overcurrent relays (P127) were included to register the current and voltage measurements. Figure 15 shows the experimental set-up.

The directional overcurrent relays (P127) are MiCom P127 type with analogue inputs for the current and voltage signals obtained from the VT's and CT's. Current transformers CT1C and CT2C measure the currents I_{A1} and I_{A2} that enter from the positive terminals in ATS1 and ATS2. Voltage transformers VT1C and VT2C measure the voltage V_C at the connection points of each ATS to the catenary. Current transformers CT1F and CT2F measure the currents that enter the ATS1 and ATS2 from the connection point to the feeder. Such currents and voltages are driven to the protection relay P127. In the protection relay P127, at ATS1, the current input assigned to phase A is connected to the current transformer CT1C, the current input assigned to phase B is not used, and the current input assigned to phase C is connected to current transformer CT1F. Voltage inputs for phases A and C are connected to the 0 V conductor, whereas the voltage input for phase B is connected to the voltage transformer VT1C. The same connections are used for ATS2 measurements.

The protection relay P127 was set to release a tripping command when the currents measured had values over the previous adjusted setting and when the angle between the voltage V_C and the currents measured by CTCs or CTFs is approximately 90°. To guarantee the correct operation of the directional overcurrent relays (P127), a range in the angle setting is required. After analysis of the experimental results, we find that an angle setting range from 60° to 120° (90° ± 30°) is appropriate. This angle range should be adapted for a particular 2 × 25 kV supply system.

When the tripping command given by the protection relay P127 is in response to the currents provided by CT1C or CT2C, the output free of potential contact RLP1 or RLP2 is activated at the corresponding P127 protection relay. This situation corresponds to a fault between the catenary and rail with high current circulating from the catenary and with an angle of about 90° between the corresponding current and voltage.

Another option for tripping commands given by the protection relay P127 is in response to the currents provided by CT1F or CT2F. Now the output free of potential contact RLN1 or RLN2 is activated. This situation corresponds to a fault between the feeder and rail with high current circulating from the feeder and an angle between such currents and the voltage V_C also close to 90°.

Figure 16 shows, as an example of one of the tests performed, a disturbance record provided by the protection relay P127 when a fault has happened between the catenary and the 0 V rail conductors. The tripping command is sent through the output contact RLP as the angle between the incoming current from the catenary and the voltage is close to 90°.

If the fault happens in the first Subsection A, the tripping command will be delivered by output contacts RLP1 or RLN1 only in the first protection relay. If the fault is located in Subsection B, protection relays 1 and 2 will activate their corresponding output contacts for tripping. Finally, if the fault is in Subsection C, only the output contacts for tripping in relay 2 will be activated. These options are listed in Table 4, where SA indicates any output that has been activated. Any output contact which is not activated is represented in Table 4 as NO.

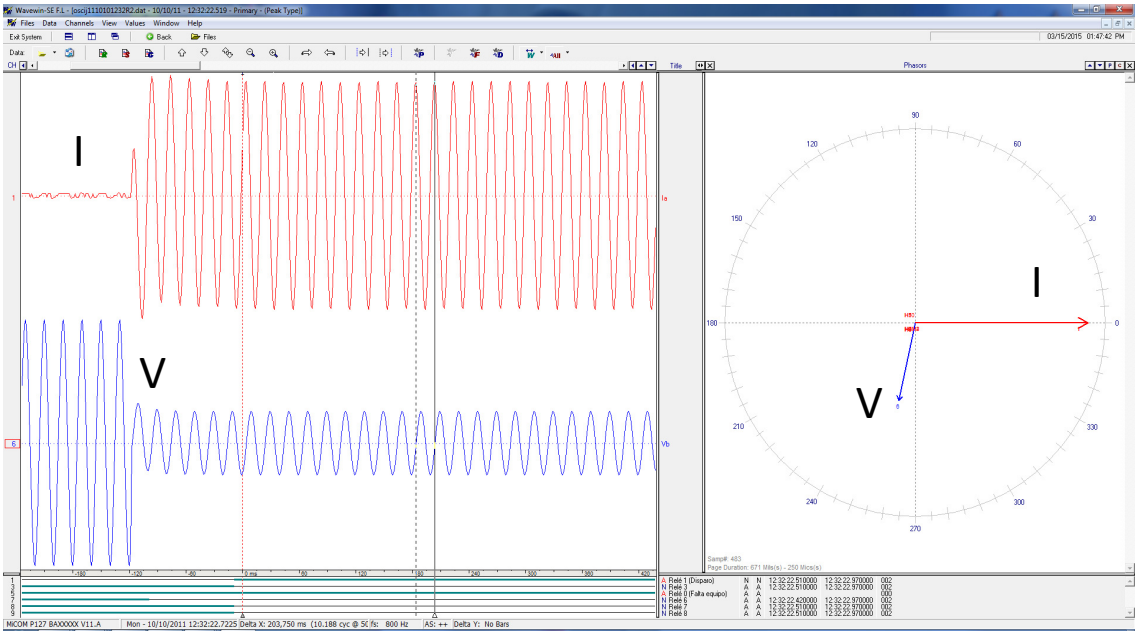

Figure 16. Disturbance record from the protection relay P127. Current and voltage in ATS during a fault between catenary and 0 V conductor.

Table 4. Activation of the output contacts of the protection relays as a function of the subsection and conductor with fault.

Fault location	RLP1	RLN1	RLP2	RLN2
Fault at catenary in Subsection A	SA	NO	NO	NO
Fault at feeder in Subsection A	NO	SA	NO	NO
Fault at catenary in Subsection B	SA	NO	SA	NO
Fault at feeder in Subsection B	NO	SA	NO	SA
Fault at catenary in Subsection C	NO	NO	SA	NO
Fault at feeder in Subsection C	NO	NO	NO	SA

Both RLP and PLN output contacts of every directional protection relay are connected to a programmable logic controller (PLC). This PLC evaluates all RLP and RLN inputs and, following the protocol described in Table 4, a signalizing message specifying which conductor and subsection have suffered the fault is sent to a PC for visualization.

6. Conclusions

A new method for identification of the subsection and conductor with a ground fault has been presented in this paper. It is suitable for 2 × 25 kV railway supply networks when the use of autotransformers makes location of the ground fault a very complex task.

This new method is based on comparison of the phase angle between currents and voltages in the catenary of each autotransformer. Depending on the value of these phase angles, it is possible to identify the subsection and the conductor with the ground fault. In other words, it is possible to know between which autotransformers the fault has occurred and if the ground fault involves the catenary or the feeder conductor.

Numerous experimental laboratory tests and MATLAB® simulations were performed, with different ground faults in all the subsections of a 2 × 25 kV model.

The results show that the phase angles between currents and voltages change in the adjacent autotransformers when a ground fault takes place between them. In the case of a ground fault on the catenary, the angle changes to 90°, and in the case of ground fault in the feeder, the angle changes to 270°. On the other hand, in the remaining autotransformers the angle remains close to 180°. In both computer simulations and laboratory tests, the results were totally satisfactory, verifying the successful operation of the method.

This new identification method, compared to traditional ground fault location methods, has the following advantages:

- It can distinguish the subsection directly after the ground fault occurs.
- No additional tests are required to locate the subsection with the ground defect.
- The feeder and the subsection affected by the ground fault can be disconnected in a short time, keeping the rest of the power system in service.
- The method is based on phase comparison, so a standard directional overcurrent relay can be used, which represents an economic advantage.

Acknowledgments

The authors wish to acknowledge the technical support of Mr. Valor, Mrs. Monje and Mr. Grollemund of Schneider Electric.

Author Contributions

Jesús Serrano has conducted in depth analysis of different ground fault detection and location systems in 2 × 25 kV railway power supply systems and developed this new method through computer simulations. Ricardo Granizo contributed the experimental set-up model, developed tests in the laboratory and compared the experimental results against the simulation results. Carlos A. Platero and Máximo López-Toledo contributed with an exhaustive review of the current protection systems installed on such railway networks. All authors have contributed to drafting and extensive revisions of the text, as well as in all the processes undertaken to test, draft and obtain the approval of the patent "System for localization of the section with ground fault in double pole railway power systems with autotransformers", with application patent No. P201430495 (3 April 2014).

Conflicts of Interest

The authors declare no conflict of interest.

Nomenclature

AC: Alternating current.
ATS: Auto-transformer station.
ATSN: Auto-transformer station at the end of Subsection N.
CT1C: Catenary current transformer in autotransformer 1.

CT2C: Catenary current transformer in autotransformer 2.
CT1F: Feeder current transformer in autotransformer 1.
CT2F: Feeder current transformer in autotransformer 2.
I: Autotransformer number: 1, 2, 3,…N.
$I_{Ai:}$ Current input from catenary in autotransformer "i".
NO: Output not activated in protection relay.
P127: Directional overcurrent protection relay.
PC: Personal computer.
PLC: Programmable logic controller.
RLN1: Output contact in protection relay of autotransformer 1 for ground fault indication in feeder.
RLN2: Output contact in protection relay of autotransformer 2 for ground fault indication in feeder.
RLP1: Output contact in protection relay of autotransformer 1 for ground fault indication in catenary.
RLP2: Output contact in protection relay of autotransformer 2 for ground fault indication in catenary.
SA: Output activated in the protection relay.
SATS: Autotransformer station at the end of the section.
V1: Voltage source 1.
V2: Voltage source 2.
$V_{Ci:}$ Catenary voltage in autotransformer "i".
VT1C: Voltage transformer in autotransformer 1.
VT2C: Voltage transformer in autotransformer 2.
X_L: Theoretical catenary inductance.
Z: Inductive impedance.
Z_C: Catenary self-impedance value per length unit.
Z_F: Feeder self-impedance value per length unit.
Z_R: Rail self-impedance value per length unit.
Z_{CF}: Mutual impedance Catenary-Feeder value per length unit.
Z_{CR}: Mutual impedance Catenary-Rail value per length unit.
Z_{FR}: Mutual impedance Feeder-Rail value per length unit.

References

1. Kneschke, T.A.; Hong, J.; Natarajan, R.; Naqvi, W. Impedance calculations for SEPTA's rail power distribution system. In Proceedings of the 1995 IEEE/ASME Joint Railroad Conference, Baltimore, MD, USA, 4–6 April 1995; pp. 79–85.
2. Pilo, E.; Rouco, R.; Fernandez, A. A reduced representation of 2 × 25 kV electrical systems for high-speed railways. In Proceedings of the 2003 IEEE/ASME Joint Rail Conference, Chicago, IL, USA, 22–24 April 2003; pp. 199–205.
3. Courtois, C. Why the 2 × 25 kV alternative? In Proceedings of the IEE Colloquium on 50 kV Autotransformer Traction Supply Systems—The French Experience, London, UK, 9 November 1993; pp. 1:1–1:4.

4. Han, Z.; Zhang, Y.; Liu, S.; Gao, S. Modeling and Simulation for Traction Power Supply System of High-Speed Railway. In Proceedings of the 2011 Asia-Pacific Power and Energy Engineering Conference (APPEEC), Wuhan, China, 25–28 March 2011; pp. 1–4.
5. Lee, B.E.; Park, J.-W.; Crossley, P.A.; Kang, Y.C. Induced Voltages Ratio-Based Algorithm for Fault Detection, and Faulted Phase and Winding Identification of a Three-Winding Power Transformer. *Energies* **2014**, *7*, 6031–6049.
6. Gao, B.; Wei, W.; Zhang, L.; Chen, N.; Wu, Y.; Tang, Y. Differential Protection for an Outgoing Transformer of Large-Scale Doubly Fed Induction Generator-Based Wind Farms. *Energies* **2014**, *7*, 5566–5585.
7. Tatietse, T.; Voufo, J. Fault Diagnosis on Medium Voltage (MV) Electric Power Distribution Networks: The Case of the Downstream Network of the AES-SONEL Ngousso Sub-Station. *Energies* **2009**, *2*, 243–257.
8. Richards, S.H. Application benefits of modern microprocessor distance protection for AC electrified railways. In Proceedings of the Sixth International Conference on Developments in Power System Protection, Nottingham, UK, 25–27 March 1997; pp. 338–341.
9. Zhou, Y.; Xu, G.; Chen, Y. Fault Location in Power Electrical Traction Line System. *Energies* **2012**, *5*, 5002–5018.
10. Chen, T.H.; Hsu, Y.F. Systematized short-circuit analysis of a 2 × 25 kV electric traction network. *Electr. Power Syst. Res.* **1998**, *47*, 133–142.
11. Alstom T&D Energy Automation & Information. *Protection of A.C. Electrified Railways. Network Protection & Automation Guide*, 1st ed.; Alstom T&D Energy Automation & Information: Levallois-Perret, France, July 2002; pp. 352–369.
12. Wang, C.; Yin, X. Comprehensive Revisions on Fault-Location Algorithm Suitable for Dedicated Passenger Line of High-Speed Electrified Railway. *IEEE Trans. Power Deliv.* **2012**, *27*, 2415–2417.
13. Xu, G.; Zhou, Y.; Chen, Y. Model-Based Fault Location with Frequency Domain for Power Traction System. *Energies* **2013**, *6*, 3097–3114.
14. Huang, Y.H.; Yong, C.; Jian, X.; Lei, T.; Jin, L. Research of implementing least squares in digital distance relaying for AC electrified railway. In Proceedings of the 2004 Eighth IEE International Conference on Developments in Power System Protection, Amsterdam, The Netherlands, 5–8 April 2004; pp. 116–118.
15. Millard, A.; Taylor, I.A.; Weller, G.C. AC electrified railways-protection and distance to fault measurement. In Proceedings of the 1995 International Conference on Electric Railways in a United Europe, Amsterdam, The Netherlands, 27–30 March 1995; pp. 73–77.
16. Han, Z.; Liu, S.; Gao, S.; Bo, Z. Protection scheme for China high-speed railway. In Proceedings of the 10th IET International Conference on Developments in Power System Protection (DPSP 2010), Managing the Change, Manchester, UK, 29 March–1 April 2010; pp. 1–5.
17. Pudney, E.; Wales, R. Optimized overhead line maintenance on 25 kV electrified railways using remotely monitored distance protection. In Proceedings of the 2001 Seventh International Conference on Developments in Power System Protection (IEE), Amsterdam, The Netherlands, 9–12 April 2001; pp. 495–498.

18. Sezi, T.; Menter, F.E. Protection scheme for a new AC railway traction power system. In Proceedings of the 1999 IEEE Transmission and Distribution Conference, New Orleans, LA, USA, 11–16 April 1999; pp. 388–393.
19. Agarwal, K.K.; Candlish, J.; Carney, T. Automatic fault location and isolation system for the electric traction overhead lines. In Proceedings of the 2002 ASME/IEEE Joint Railroad Conference, Washington, DC, USA, 23–25 April 2002; pp. 117–122.
20. Wedepohl, L.M.; Jackson, L. Modified nodal analysis: An essential addition to electrical circuit theory and analysis. *Eng. Sci. Educ. J.* **2002**, *11*, 84–92.